NANO LETTERS

2008
Vol. 8, No. 8
2564-2569

Superaligned Carbon Nanotube Grid for High Resolution Transmission Electron Microscopy of Nanomaterials

Lina Zhang,*,† Chen Feng,† Zhuo Chen, Liang Liu, Kaili Jiang,* Qunqing Li, and Shoushan Fan

Department of Physics and Tsinghua-Foxconn Nanotechnology Research Centre, Tsinghua University, Beijing 100084, People's Republic of China

Received May 5, 2008

ABSTRACT

Nano is one of the hottest topics in current science and technology. Characterizations of nanomaterials by high resolution transmission electron microscopy (TEM) are becoming indispensable today. To gain better performance of TEM, people are expecting a novel TEM grid of which the supporting film should be highly conductive, ultrathin but robust, and preferably nanoholey. Here we report a method of mass producing such a kind of carbon nanotube TEM grids. The supporting films are made by cross stacking ultrathin superaligned carbon nanotube films, resulting in a large number of nanosized holes and numerous effective edges. Together with the robustness, good conductivity, and strong adsorbability inherited from carbon nanotubes, these TEM grids show much better performance than conventional amorphous carbon grids.

With rapidly development of nanoscale science and technology, techniques capable of structural characterization on the nanometer scale have central importance. High-resolution transmission electron microscopy (HRTEM) technique has played a key role in the discovery and characterization of nanomaterials. In addition to well TEM system, to get a perfect HRTEM image, the technique of specimen preparation is important. Generally, for preparing a TEM specimen of nanopowders, TEM microgrid is used, and the powders are dispersed on the surface of the grid which coated with thin carbon or holey carbon film.[1–8] But for small particles with a size comparable to the thickness of the supporting film, especially those less than 5 nm in diameter, it is difficult to gain clear HRTEM images due to the influence of scattering from the amorphous carbon film of the support grid. To overcome this difficulty, efforts improving the construction of the supporting grid have been researched. Ultrathin carbon supporting films have been developed[9] but the interference from the supporting film still remains. To obtain clear HRTEM images of nanomaterials, especially nanoparticles, a supporting film, which is conductive, ultrathin but robust, and preferably nanoholey, is expected.

In 2002, we developed a method for synthesizing superaligned carbon nanotube (SACNT) arrays, from which continuous films composed of unidirectional carbon nanotubes can be directly spun.[10–12] The SACNT arrays (SACNTA) are distinguished from ordinary vertically aligned CNT arrays by their "super-aligned" nature, i.e., the CNTs in SACNTAs have a much better alignment than those in ordinary arrays, which is a consequence of narrower diameter distribution and higher nucleation density.[10,11] In 2005, we scaled up the synthesis in a 4 in. low pressure chemical vapor deposition (LP-CVD) system. Recently we have achieved a batch growth of 4 in. SACNTAs in a 6 in. LP-CVD system. One wafer of SACNT array can be directly converted to a continuous film which is 8−10 cm by 60 m with a thickness of tens of nanometers. These yarns are transparent and highly conductive, which is distinguished from random CNT films by their "unidirectional" nature, i.e., in which the CNTs are parallel-aligned in the drawing direction and end-to-end jointed to form a continuous thin film. Many potential applications for these have been demonstrated, including polarizers, transparent conducting films, and polarized light sources etc.[10–13]

In this paper, we show that these SACNT films are able to meet all the aforementioned requirements for a supporting film of TEM grids. Then included as a supporting film, the grids with it show an improved performance than that with amorphous carbon supporting film, especially for characterizing nanoparticles. More importantly, the fabrication process demonstrated here can be fully automatic with very high production rates, which is suitable for batch production.

* Corresponding authors. E-mail: (L.Z.) zhanglina@tsinghua.edu.cn; (K.J.) JiangKL@tsinghua.edu.cn.
† These authors contributed equally to this work.

10.1021/nl8012727 CCC: $40.75
Published on Web 07/09/2008

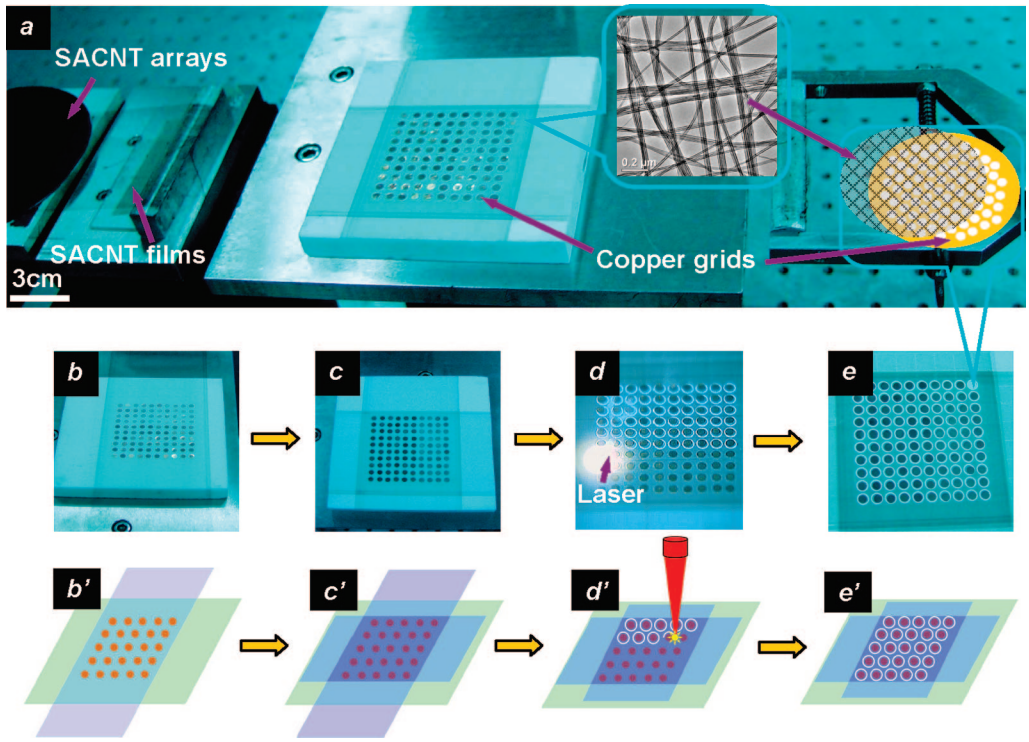

Figure 1. Schematic of fabrication process of superaligned carbon nanotube (SACNT) grids. (a) Optical image showing copper grid arrays being covered with SACNT films (insert: TEM magnified micromorphology of four layers of films). (b,b′) Copper grid arrays covered with a layer of SACNT films. (c,c′) Copper grid arrays covered with four cross-stacking layers of SACNT films. (d,d′) A laser beam ablating the part of SACNT films around copper grids. (e,e′) The finished SACNT-grids (insert: a magnified sketch map of a finished SACNT-grid).

The SACNTAs used in this paper were synthesized in batches on a 4 in. silicon wafer with iron as a catalyst in a 6-in. LP-CVD system.[10,11] The SACNT films can be directly drawn out from the SACNT array as shown in Figure 1a and in the Supporting Information. The fabrication of the SACNT film based TEM grids is a four-step process as shown in Figure 1b∼1e (Figure 1b′∼1e′ are their sketch maps correspondingly). (1) The copper grids (400 mesh, ∅3 mm each) were arranged on a ceramic, quartz, or metal substrate into a grids array. Then SACNT films, 8 cm in width, were drawn from a sidewall of the SACNT arrays, and pressed onto the copper grids arrays (Figure 1b,b′). (2) Four layers of SACNT films were cross-stacked layer by layer (Figure.1c,c′). Then an organic solvent such as ethanol was dispensed on it, after which the SACNT films attached to the copper grid tightly. (3) After step 2, we had an array of SACNT-copper grids, which were interconnected by SACNT films. The copper grids arrays covered with SACNT films were then put under a scanning focused laser system which had been utilized to direct write CNTs[14] and activate CNT field emitters.[15] The focused laser beam scanned the predefined circle patterns around each grid. The CNTs on the tracks of the focused laser beam were burned out, resulting in the separation of grids (see Figure.1d,d′ and Supporting Information). (4) Finally the SACNT-grid was finished, which was composed of a copper grid base and a SACNT supporting film (Figure.1e,e′). The prepared grids arrays can be picked up and collected for packaging. This process enables the efficient fabrication of the grids in batches. In the demonstration shown in Figure 1, one hundred SACNT-grids can be fabricated within a few minutes.

Following conventional methods to prepare TEM specimen of nanoparticles using the SACNT-grids, nanopowders, nanowires, and nanotubes can be dispersed in alcohol by ultrasonic agitating, and then by dropping the suspended solution onto the grids. For some monodispersed nanoparticle solution systems, we can drop the solution onto the grid directly. In this work, we prepared TEM specimens of nanomaterials to include Au, BN, and Cu_2S using these SACNT-grids. TEM observations were carried out using a FEI Tecnai G2 F20 TEM at 200 kV accelerate voltage.

Figure 2a shows a scanning electron microscopy (SEM) image of a SACNT-grid. In Figure 2b, the SEM image at a higher magnification indicates the present of an ultrathin SACNT film covering the copper grid base. Upon closer magnification (Figure 2c), we can see that the CNTs are interweaved together forming a SACNT gauze which is a quasi regular network with numerous holes in small sizes. By our statistic analysis, the holes are mostly less than 1 μm in diameter, and the nanometer-sized holes are more than 60% of all holes. Considering the good electric conductivity and mechanical strength of CNTs, this SACNT-grid is expected to be the ideal candidate for the characterization of nanomaterials. To test this point, we performed a series of HRTEM investigations on nanoparticles and nanotubes supported by SACNT-grid.

Figure 3 shows the TEM images of the Au nanoparticles and BN nanotubes supported by the SACNT-grid. From

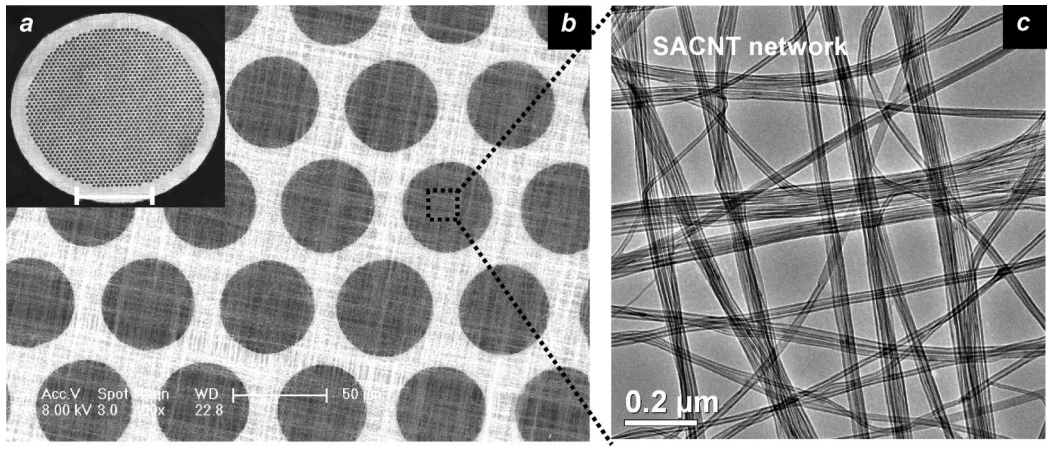

Figure 2. Morphologies of a SACNT-grid. (a) A SEM full view image of a SACNT-grid (the scale bar represents 1 mm length). (b) Image of the SACNT gauze over the holes of the copper grid base (local magnification of panel a). (c) Image of the carbon nanotube gauze covering a hole showing a network morphology (local magnification of panel b).

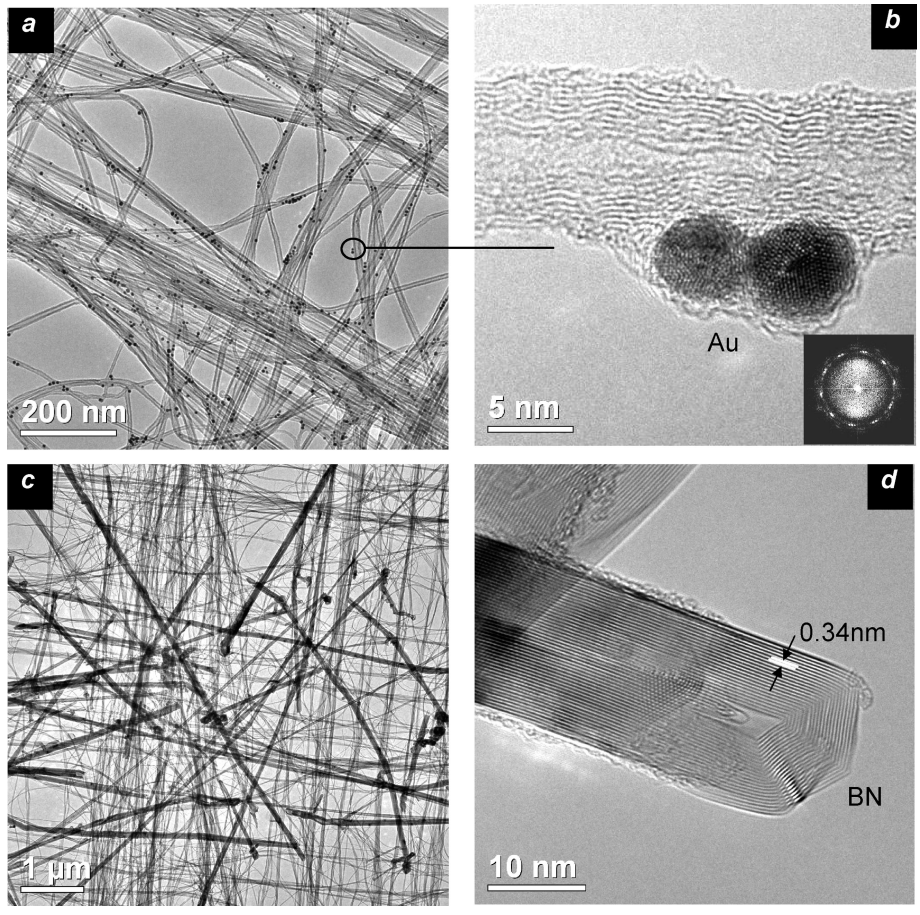

Figure 3. TEM images of Au nanoparticles and BN nanotubes using SACNT-grids. (a) Low magnification TEM image of Au nanoparticle dispersed on a SACNT supporting network showing Au particles located on sides of CNTs (black dots represent Au nanoparticles). (b) HRTEM image of two Au particles on a side of a carbon nanotube (inset: diffraction pattern by FFT). (c) A low magnification TEM image of BN nanotubes dispersed on a SACNT supporting network (black wires represent BN nanotubes). (d) HRTEM image of a BN nanowire over a hole of the SACNT gauze.

Figure 3a, we can see that many black dots randomly rest on the edges of nanoholes, which are the Au nanoparticles adhering to the sidewalls of CNTs. During TEM experiments, these suspended nanoparticles were stable under the irradiation of the electron beam, the HRTEM images can be easily obtained without supporting disturbance. Figure 3b shows the HRTEM lattice image of Au nanoparticles (corresponding to the site marked by a circle in Figure 3a). The diffraction pattern obtained from fast Fourier transformation (FFT) shows polycrystalline microstructure of the Au particles.

Figure 3c shows a low magnification TEM image of BN nanotubes on a SACNT-grid. The randomly distributed BN

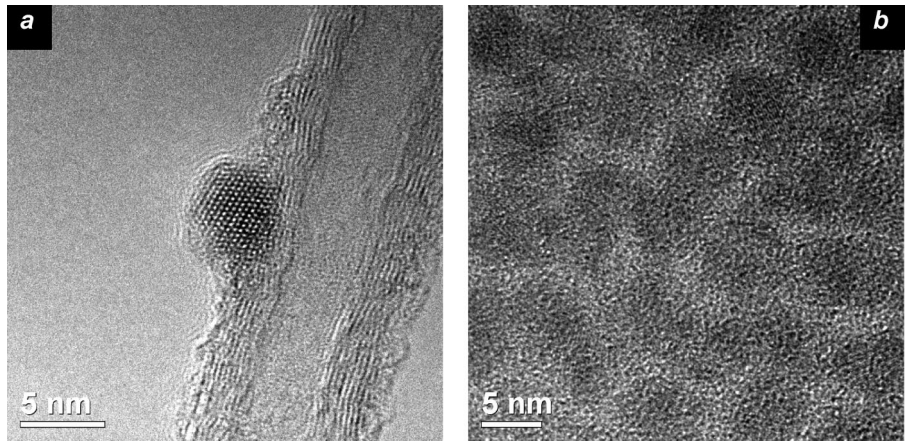

Figure 4. Comparison between TEM images of monodispersed Cu_2S nanoparticles/oleic alcohol on different grids. (a) HRTEM image of a Cu_2S nanoparticle on one side of a nanotube (using a SACNT-grid). (b) Image of Cu_2S particles on an amorphous carbon film (using a conventional amorphous carbon grid).

nanotubes can easily be discerned from the nearly aligned supporting CNTs due to its different electric conductivity and mechanical flexibility. Due to the good electric conductivity and mechanical stability of SACNT gauzes, very clear HRTEM lattice images of a BN nanotube can be readily obtained (Figure 3d).

We prepared TEM specimens of monodispersed Cu_2S particles/oleic alcohol by SACNT-grid and conventional holey amorphous carbon microgrid respectively, and then took an HRTEM image under same acquisition conditions as before. The experimental results are shown in Figure 4. HRTEM image of Figure 4a, shows a clearer profile and fine structures of individual particles of Cu_2S by using SACNT-grid. When compared to the case of the traditional grids as shown in Figure 4b, it seems that the carbon nanotube network can "catch" a single Cu_2S nanoparticle from a pile of monodispersed Cu_2S nanoparticles which were enwrapped by oleic alcohol. Thus double disturbance from both amorphous supporting film and organic activator can be avoided when the particle was observed under TEM.

In comparison with conventional holey amorphous carbon grid, the new SACNT-grid has several advantages due to its novel structure and intrinsic properties of carbon nanotubes.

For a conventional holey amorphous carbon microgrid, its supporting film is usually an amorphous carbon film with randomly distributed circular holes. In order to illuminate the distinct features due to the structure variety of the SACNT-grid, we may describe a supporting film of TEM grid according to the conventional microgrid as three parts: supporting part, holes, and the edges along the holes.

Compared to a conventional holey amorphous carbon microgrid, the SACNT-grid has a different structure. In the supporting film of a SACNT-grid, the carbon nanotubes interweave together forming a nearly regular network. So, accordingly, the amorphous carbon supporting part of the conventional microgrid here changes into a carbon nanotube net framework, the random circular holes change to be nearly regular rectangular apertures, and the edges of amorphous carbon film along circular holes change into sides of carbon nanotubes along the holes. This new structure of SACNT-grids leads to few supporting areas, an substantial increase in the number of holes but also a drastic reduction in hole sizes, and hence a large number of edges. All of these factors result in several novel features in application uses.

For small nanoparticles, especially those less than 5 nm in diameter, the phase contrast is the main mechanism during TEM imaging. These particles usually have two positions on the conventional holey amorphous carbon grid, lying on the supporting film or adhered to the edges of the holes. In the former case, during TEM imaging the scattering from the amorphous carbon supporting film can easily disturb or overwhelm the contrast due to nanoparticles, making the observation of fine structure and contour of nanoparticles very difficult. When the particles are smaller, the influence of scattering from supporting films is increased, and this causes the HRTEM images of the small nanoparticles to become increasing unclear. For the latter case, the nanoparticle is a "clean" sample, and there is no effect from the supporting film, which we can observe the fine structure without difficulty. This is the ideal condition we want to obtain during TEM observations, especially HRTEM. Unfortunately, the ratio between the holes edges length and supporting film area is too small to let these scarce particles have a chance to be on the edge in general.

Our SACNT-grid can overcome the difficulties as aforementioned. SEM and TEM results show that the size range of the holes, i.e., apertures of the gauze, which include four layers of SACNT films, is from several to hundreds of nanometers, and the nanometer-sized holes are more than 60% of all holes. The hole sizes can be smaller with the increase of layers of SACNT films. Hence the gauze can support particles sizes from nanometers to micrometers. Furthermore, the enormously increased holes with smaller hole sizes can result in that nanomaterials such as nanowires and nanorods and such have a greater chance to be suspended on the edges of holes and to be the "clean object" with more ease. More importantly, in the same areas of a supporting film, the SACNT gauze has far more edges than the conventional one. From the TEM observations, each individual carbon nanotube can provide two edges−sides of the

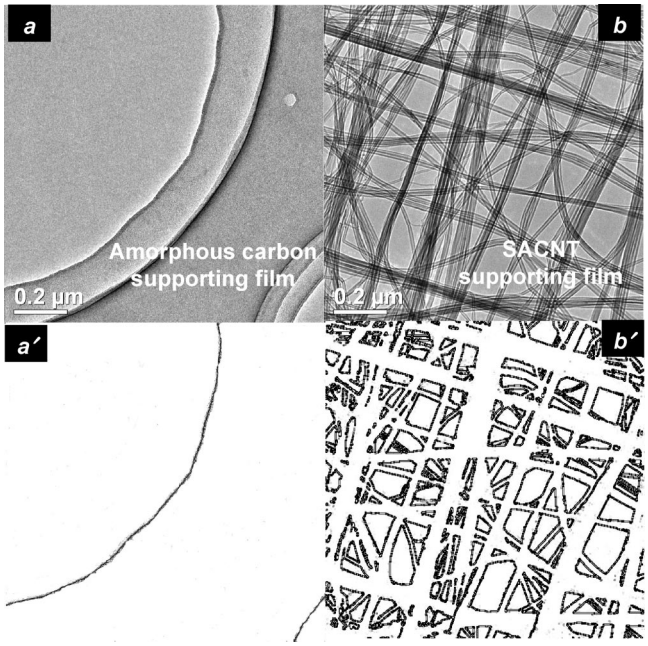

Figure 5. Comparison of number and length of effective edges between two kinds of grids. (a) TEM image of a local amorphous carbon supporting film of a conventional holey carbon microgrid. (a′) Schematic lines of effective edges of the supporting film extracted from panel a (dark lines represent edges). (b) TEM image of a local SACNT supporting film of a SACNT grid. (b′) Schematic lines of effective edges of the supporting film extracted from panel b (dark lines represent edges).

nanotube. Figure 5 shows the TEM morphology of a conventional supporting film (Figure 5a) and a SACNT supporting film (Figure 5b) at same magnification. Black lines in Figure 5a′,b′ represent effective edges of the supporting films extracted from Figure 5a,b, respectively. According to Figure 5a′,b′, the difference of edge numbers between two kinds of supporting film is obvious. Statistical results show that the length value of the edges in new grid is about one order larger than the conventional grid. So for small nanoparticles, when they are dispersed on the SACNT-grid, they have far more opportunities to locate on the edges, i.e., the sides of carbon nanotubes (as shown in Figure 3a). Thus we can obtain the "clean" samples easily and conveniently perform TEM observation, especially HRTEM of them without supporting disturbance.

In addition to the novel features mentioned above which originated from the structure of the new SACNT-grid, there are also several advanced characteristics resulting from the excellent intrinsic physical properties of carbon nanotubes. First, the carbon nanotube has strong adsorbability, and it can easily adsorb small particles and ensure them to be suspended stably during TEM observation. Second, due to good conductivity of multiwall carbon nanotubes, the superaligned carbon nanotube film also has good electrical conductivity. We measured the sheet resistivity of the four layers SACNT film with 4 point probe Rs mapping tool (CDE Resmap) and estimated that the bulk resistivity is about 3.8×10^{-4} Ω•m. This is enough for TEM observations. Third, because of the certain interspace between sidewalls of the MWCNTs, 0.34nm, the carbon nanotube grid can be a standard sample for calibration of TEM magnification and size measurement of specimens. In Figure 3b, for example, according to the interspace between sidewalls of the nanotube, we can measure the diameter of the two gold particles. Lastly, because of the regular structure and purity of the superaligned carbon nanotube, the crystal lattice image of interested particles can not be interruptive.

Besides being a supporting film for TEM characterization, SACNT-grids can be a carrier for nanoparticles synthesis, nanosized catalysts, and quantum dots array due to its intrinsic network structure and properties. It can also be helpful to investigate the interaction between special nanoparticles and carbon nanotubes.

In summary, we have fabricated a new kind of grid using carbon nanotube films as a supporting film for TEM. The supporting films are made by cross stacking ultrathin superaligned carbon nanotube films, resulting in a large number of nanosized holes and numerous effective edges. Besides the novel structure, the film is a good conductor and has a strong adsorbability inherited from the carbon nanotubes. Clear high-resolution images without support disturbance of different nanoparticles and nanotubes were obtained conveniently. It has a distinct advantage when characterizing the fine structure of nanomaterials as compared with conventional holey amorphous carbon grid, especially for small nanoparticles. The fabrication process of the SACNT-grids is fully automatic with very high production rates, which is a batch production process.

Acknowledgment. The authors thank Professor Li Yadong and Dr. Zhuang Zhongbin for providing Cu_2S nanoparticles and Professor Tang ChengChun for providing BN nanotubes. This work was financially supported by the National Basic Research Program of China (2005CB623606, 2007CB935301) and NSFC (10704044).

Supporting Information Available: One video named "CNTgrids.qt" shows the fabrication process of the CNT grids, including the process of cross stacking ultrathin superaligned carbon nanotube films onto the surface of copper grids and ablating CNTs along the predefined circle patterns around each grid by focused laser beam. This material is available free of charge via the Internet at http://pubs.acs.org.

References

(1) Yao, N.; Wang, Z. L. *Handbook of Microscopy for Nanotechnology*; Tsinghua University Press: Beijing, 2005.
(2) Guo, K. X.; Ye, H. Q. *The Application of HREM in Solid State Science*; Science Press: Beijing, 1985.
(3) Zhu, J.; Ye, H. Q.; Wang, R. H.; Wen, S. L.; Kang, Z. C. *Analytical Electron Microscopy with High Spatial Resolution*; Science Press: Beijing, 1987.
(4) Smith, D. J. *Rep. Prog. Phys.* **1997**, *60*, 1513.
(5) Ye, H. Q.; Wang, Y. M. *Progress in Transmission Electron Microcopy*; Science Press: Beijing, 2003.
(6) Wang, Z. L.; Hui, C. *Electron Microscopy of Nanotubes*; Tsinghua University Press: Beijing, 2004.
(7) Chester, D. W.; Klemic, J. F.; Stern, E.; Sigworth, F. J.; Klemic, K. G. *Ultramicroscopy* **2007**, *107*, 685.
(8) Choi, Y.; Johnson, J.; Moreau, R.; Perozziello, E.; Ural, A. *Nanotechnology* **2006**, *17*, 4635.

(9) Kim, Y. M.; Kang, J. S.; Jeung, J. M.; Ko, Y. C.; Kim, Y. J. *Microsc. Microanal.* **2005**, *11* (Suppl 2), 2106.
(10) Jiang, K. L.; Li, Q. Q.; Fan, S. S. *Nature* **2002**, *419*, 801.
(11) Zhang, X. B.; Jiang, K. L.; Feng, C.; Liu, P.; Zhang, L. N.; Kong, J.; Zhang, T. H.; Li, Q. Q.; Fan, S. S. *Adv. Mater.* **2006**, *18*, 1505.
(12) Liu, K.; Sun, Y. H.; Chen, L.; Feng, C.; Feng, X. F.; Jiang, K. L.; Zhao, Y. G.; Fan, S. S. *Nano Lett.* **2008**, *8*, 700.
(13) Zhang, M.; Fang, S. L.; Zakhidov, A. A.; Lee, S. B.; Aliev, A. E.; Williams, C. D.; Atkinson, K. R.; Baughman, R. H. *Science* **2005**, *309*, 1215.
(14) Chen, Z.; Wei, Y.; Luo, C. X.; Jiang, K. L.; Zhang, L. N.; Li, Q. Q.; Fan, S. S. *Appl. Phys. Lett.* **2007**, *90*, 133108.
(15) Chen, Z.; Zhu, F.; Wei, Y.; Jiang, K. L.; Liu, L.; Fan, S. S. *Nanotechnology* **2008**, *19*, 135703.

NL8012727